DOI: 10.1002/chem.200700205

Understanding Adsorption and Interactions of Alkane Isomer Mixtures in Isoreticular Metal–Organic Frameworks

Li Zhang, Qi Wang,* Tao Wu, and Ying-Chun Liu[a]

Abstract: Novel metal–organic frameworks (MOFs) may lead to advances in adsorption and catalysis owing to their superior properties compared to traditional nanoporous materials. A combination of the grand canonical Monte Carlo method and configurational-bias Monte Carlo simulation was used to evaluate the adsorption isotherms of C_4–C_6 alkane isomer mixtures in IRMOF-1 and IRMOF-6. The amounts of adsorbed linear and branched alkanes increase with increasing pressure, and the amount of branched alkanes is larger than that of the linear ones. The locations of the alkane isomer reveal that the Zn_4O clusters of the IRMOFs are the preferential adsorption sites for the adsorbate molecules. The interaction energy between the Zn_4O cluster and the adsorbate is larger than that between the organic linker and the adsorbate. It was further confirmed that the Zn_4O cluster plays a much more important role in adsorption by pushing a probe molecule into the pore at positions closer to the Zn_4O cluster. It is difficult for branched alkane molecules to approach the Zn_4O cluster of IRMOF-6 closely owing to strong spatial hindrance. In addition, the adsorption selectivity is discussed from the viewpoints of thermodynamics and kinetics, and the diffusion behavior of *n*-butane and 2-methylpropane were investigated to illustrate the relationship between diffusion and adsorption.

Keywords: adsorption · alkanes · metal–organic frameworks · microporous materials · molecular dynamics

Introduction

In recent years, metal–organic framework (MOF) materials have been considered as promising alternatives to zeolites and other nanoporous materials for adsorption,[1,2] separation,[3,4] and catalysis.[5] Compared with zeolites and activated carbons, MOFs can be designed to produce various materials with different pore sizes and functionalities,[1,2] due to the variety of possible linker molecules and metal–organic complexes. An outstanding property of MOFs is their gas storage, especially for fuel gases such as hydrogen, methane, and carbon monoxide. Owing to their high storage capacity, much research has been devoted to synthesizing novel MOFs and studying their adsorption behavior.[6–10] On the other hand, the adsorption and separation behaviors of alkane isomers in microporous materials are of great importance to industrial applications. However, it is time-consuming to obtain adsorption data by experiments alone, especially for mixtures. Molecular simulation provides an attractive way to acquire adsorption data, but most of these works focused on the adsorption and diffusion of hydrogen and some other light gases in MOFs and isoreticular MOFs (IRMOFs). For example, Vishnyakov et al.[11] simulated the adsorption isotherm of Ar in Cu-BTC MOF, and Skoulidas[12] computed the self- and transport diffusion coefficients for Ar in Cu-BTC MOF. Similarly, Skoulidas et al.[13] studied the diffusion behavior of Ar, H_2, CH_4, CO_2, and N_2 in MOF-5 (also known as IRMOF-1), and the diffusion of Ar in MOF-2, MOF-3, and Cu-BTC MOF was assessed. Garberoglio et al.[14] investigated the adsorption of hydrogen at 77 and 298 K in IRMOF-1, -6, -8, and -14; MOF-2; and MOF-3. Yang and Zhong[15] calculated the hydrogen adsorption and diffusion behavior in IRMOF-1, -8, and -18, and further discussed the adsorption sites for hydrogen. However, only a few studies on adsorption and diffusion behaviors of alkanes in MOFs have been made, and most of them were centered on pure short-chain alkanes. Düren et al.[16] computed the adsorption isotherm for CH_4 in IRMOF-1 and IRMOF-6 with UFF and Dreiding force fields, and the results were in good agreement with experiment. They also investigated the adsorption behavior and selectivity of CH_4/*n*-C_4H_{10} mix-

[a] Dr. L. Zhang, Prof. Q. Wang, Prof. T. Wu, Dr. Y.-C. Liu
Department of Chemistry
Zhejiang University
Hangzhou 310027 (P.R. China)
Fax: (+86) 571-8795-1895
E-mail: qiwang@zju.edu.cn

tures in different IRMOFs, and proposed some newly designed materials that show higher selectivity. It was suggested that MOFs are potential materials for separation of hydrocarbons.[3] Furthermore, they calculated the self-diffusion coefficients of several alkanes in IRMOF-1 by molecular dynamics (MD) simulation, albeit at low loadings.[17] Although the adsorption behavior of alkanes such as methane and propane has been discussed, knowledge on the adsorption of alkane mixtures, especially of the longer chain alkanes and their isomers, is still lacking. In this work, the adsorption isotherms of binary mixtures of C_4–C_6 alkane isomers in IRMOF-1 and IRMOF-6 were investigated, and the locations of alkanes in these IRMOFs explored.

The diffusion behavior is of importance to assess the potential of the nanoporous materials over the full range of separation process. However, information on transport in MOFs is extremely rare; hence, it is necessary to evaluate diffusion coefficients inside MOFs and to further understand the relationship between diffusion and adsorption. Owing to experimental limitations, MD simulations were employed to obtain diffusion properties in MOFs,[13–15,17] but most of these studies focused on pure gases such as hydrogen, methane, and *n*-pentane, only a few studies were concerned with the diffusion of alkane isomer mixtures in MOFs, and the relationship between diffusion and adsorption is still poorly understood. In this work, self-diffusion coefficients in mixtures for *n*-butane and 2-methylpropane in IRMOF-6 and IRMOF-1 were evaluated, and the number density profiles and the residence times for *n*-butane and 2-methyl propane molecules around the Zn_4O cluster of IRMOF-6 were also calculated to investigate the relationship between diffusion and adsorption.

Model and Simulation Details

In our previous works,[18,19] we used the grand canonical Monte Carlo (GCMC) method in combination with the configurational-bias Monte Carlo (CBMC) technique to compute adsorption isotherms for pure components and mixtures of linear alkanes and their isomers in different zeolites. In this work, we used GCMC/CBMC to investigate the adsorption behavior and interactions of C_4–C_6 alkane isomers in IRMOF-1 and IRMOF-6.

The interactions between the adsorbate molecules and between the MOF frameworks and the adsorbate molecules were described with Lennard–Jones potentials. The atomistic model was employed for MOF frameworks, but the adsorbate molecules were described with a united atom (UA) force field. The potential parameters for alkane molecules were taken from Vlugt et al.,[20] while for the MOF frameworks the Dreiding force field[21] was employed. The cutoff radius was taken to be 13.8 Å, and the cross-interaction parameters between different units were calculated from Jorgensen's mixing rules [Eqs. (1) and (2)]:[22]

$$\varepsilon_{ij} = \sqrt{\varepsilon_{ii}\varepsilon_{jj}} \quad (1)$$

$$\sigma_{ij} = \sqrt{\sigma_{ii}\sigma_{jj}} \quad (2)$$

The CBMC algorithm proposed by Smit et al.[23] combined with GCMC could be applied well to calculate the adsorption isotherm of alkanes and their mixtures. In the simulation scheme, five types of trial moves were included: moving a molecule, rotating a molecule, partly regrowing a molecule, inserting/removing a molecule, and changing the molecule identity. The details of these moves were described in ref. [18]. The GCMC simulations were carried out at 298 K, and around 2×10^5 MC cycles were performed for alkane isomer mixtures. 1×10^5 simulation steps were performed for equilibration, and another 1×10^5 steps to sample the data. The result of the simulation is the absolute amount of adsorbed molecules, while the experimentally measured value is the excess amount of adsorbed molecules. The amount of excess molecules n^{ex} is related to that of the absolute adsorbed molecules n^{abs}, the pore volume of adsorbent V^g, and the bulk gas density of adsorbed molecules ρ^g [Eq. (3)]:

$$n^{ex} = n^{abs} - V^g\rho^g \quad (3)$$

where V^g is obtained from ref. [16] and ρ^g is calculated with the Peng–Robinson equation of state.

The self-diffusion coefficients of adsorbed molecules were calculated using MD. The force fields employed in the GCMC simulations were also used in the MD simulations for consistency. Periodic boundary conditions were applied in all three dimensions, and the Beeman algorithm for integration of the equations of motion was employed. The initial configuration for MD simulation was taken from the last configuration of the previous GCMC simulation. The MD simulation was performed in the *NVT* ensemble, and the temperature was set to 298 K. The time step was set to 1 fs, and runs of 10^6 time steps were used for statistics of the properties. The self-diffusion coefficient D_A was calculated by means of the MSD of the molecules of species A [Eq. (4)]:

$$D_A = \frac{1}{6}\lim_{t\to\infty}\frac{\partial}{\partial t}\left\langle\frac{1}{N_A}\sum_{i=1}^{N_A}[r_{Ai}(t)-r_{Ai}(0)]^2\right\rangle \quad (4)$$

Results and Discussion

Comparison with experiment: The adsorption isotherms of pure components in zeolites and in some MOFs have already been simulated.[14,15,24–26] To further verify the model and the programs used in this work, the adsorption data for pure methane in IRMOF-6 were calculated at 298 K and compared with experimental data of Yaghi et al.[1] As shown in Figure 1, the simulated data agree well with experiment, that is, the simulation model is able to describe the adsorption behavior of alkanes adsorbed in MOFs.

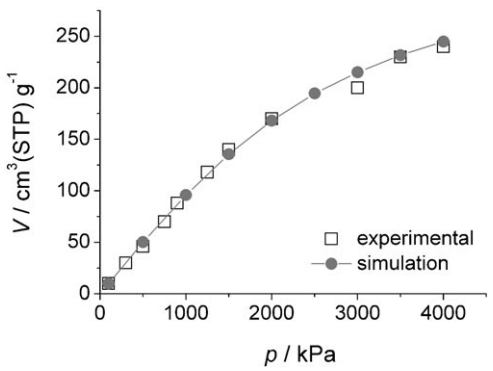

Figure 1. Comparison of the simulated adsorption isotherm for methane with experiment in IRMOF-6 at 298 K.

Adsorption and selectivity: The adsorption data of mixtures at a series of pressures are of great importance to applications in industry. However, experimental measurement of adsorption isotherms is more time-consuming for mixtures than for a pure component. In this work, the model and simulation algorithms were verified by the experimental data of methane and employed to simulate isomer mixtures. The GCMC simulations were performed on IRMOF-1 and IRMOF-6 at 298 K, and the composition of the gas mixtures was set to be 0.5 (mole fraction) for all the mixtures. Eight unit cells ($2\times2\times2$) of IRMOF-1 (-6) were used to construct the simulation box. The adsorption isotherms of C_4–C_6 alkane isomer mixtures in IRMOF-1 are plotted in Figure 2. The adsorbed amounts of branched alkanes are similar to those of linear alkanes for all the mixtures at low pressures, which is similar to the adsorption behavior in the zeolites discussed in our previous work.[19] The adsorption of both linear and branched alkanes increases to saturation with increasing pressure, and the adsorbed amounts of the linear alkanes and their isomers start to increase at almost the same pressure, which is a little different from that in MFI zeolites. Owing to the small pore size of MFI and stronger repulsive interaction, the branched alkanes seem to be squeezed out by the linear alkanes at higher pressures. However, since the pore size is as large as 9.4 Å for IRMOF-1, both the linear and branched alkanes could coexist even at very high pressure. The adsorption isotherms of C_4–C_6 alkane isomer mixtures in IRMOF-6 are presented in Figure 3. The adsorbed amounts of branched alkanes are

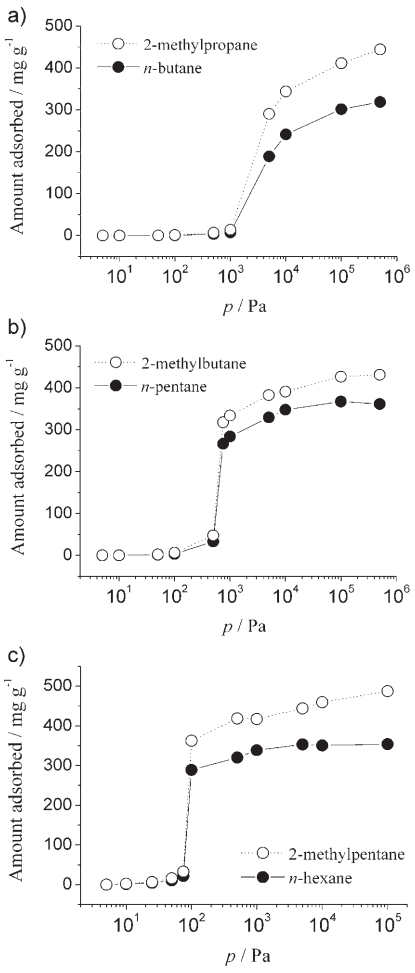

Figure 2. Adsorption isotherms of 0.5/0.5 mixtures of a) *n*-butane/2-methylpropane, b) *n*-pentane/2-methylbutane, and c) *n*-hexane/2-methylpentane at 298 K in IRMOF-1.

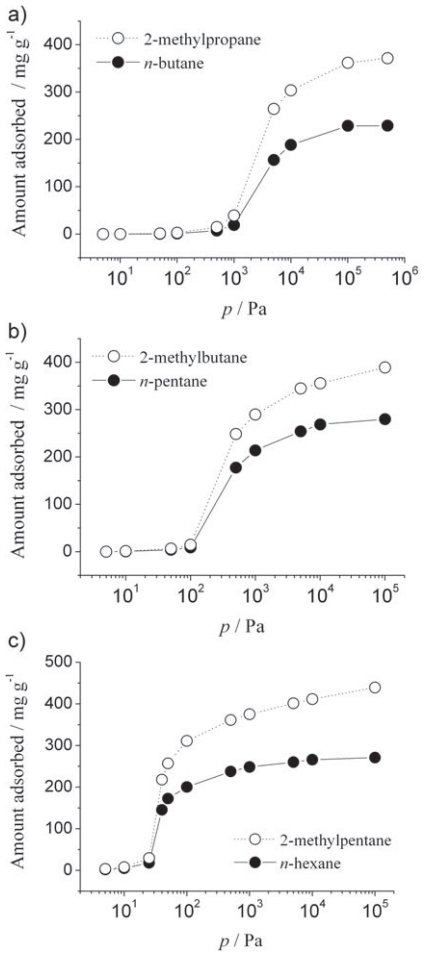

Figure 3. Adsorption isotherms of 0.5/0.5 mixtures of a) *n*-butane/2-methylpropane, b) *n*-pentane/2-methylbutane, and c) *n*-hexane/2-methylpentane at 298 K in IRMOF-6.

larger than those of the linear alkanes, as can be seen in Figures 2 and 3. Owing to hindrance by the organic linker of IRMOF-6, the adsorbed amount of alkane isomer mixtures in IRMOF-1 is a little larger than that in IRMOF-6. The difference in adsorbed amount between branched and linear alkanes in IRMOF-6 is larger than in IRMOF-1; in other words, the separation capability of IRMOF-6 may be somewhat better than that of IRMOF-1.

In separation processes, the most important factor is the relative selectivity of the adsorbent for the different components, which is defined as the ratio product of molar fractions of components A to B in the adsorption phase and in the gas phase. In this work, the relative selectivities of two

IRMOFs for 0.5 (mole fraction) mixtures were calculated (Figure 4). The result reveals that IRMOF-1 and IRMOF-6 have similar selectivities for mixtures of C_4–C_6 alkane isomers. Due to the large pore size of IRMOFs, linear and

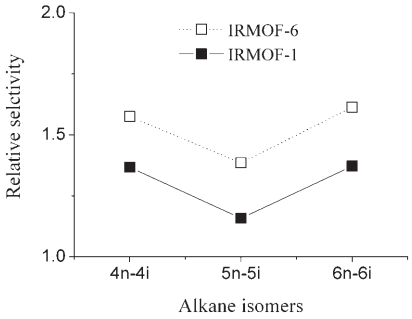

Figure 4. Relative selectivity of IRMOF-1 and IRMOF-6 for C_4–C_6 linear alkanes and their isomers (0.5/0.5 gas phase) at 298 K and 100 kPa.

branched alkanes can coexist in the pore space even at high pressure, so the selectivity of IRMOF-1 and IRMOF-6 is not as high as expected, and it is lower than that of some narrow-pore zeolites with appropriate pore sizes matching the alkane molecular sizes.[18,27,28] Figure 4 shows that the selectivity of IRMOF-6 is slightly better than that of IRMOF-1, which may be attributed to larger 3D spatial hindrance between IRMOF-6 and alkane isomers. It implies that the separation capability of IRMOFs could be improved by introducing organic linkers with greater hindrance or by adjusting the pore size to match the alkane isomer molecules by making use of framework interpenetration and/or interweaving. For example, Chen et al. showed that MOF-508 with 1D pores of 4.0×4.0 Å can be used to sieve alkane mixtures.[29] They also suggested that the specific interaction between the analytes and the organic moieties of MOFs might further enhance their separation capabilities. The interaction between alkane isomers and MOFs is discussed further below.

Location: It is of great importance to understand the adsorption sites and the locations of the molecules adsorbed in MOFs to design new MOF materials with higher storage capacity or good selectivity. As an example, the probability distribution of *n*-butane and 2-methylpropane at different pressures in IRMOF-1 are plotted in Figure 5. The center of mass of a molecule was calculated every 100 MC steps, and the position was plotted as a dot in the figure. This procedure was repeated until 10000 dots had been plotted. The framework structure of IRMOF-1 was superimposed in Figure 5. The adsorption mechanism for alkanes in IRMOFs is as follows: the *n*-butane and 2-methylpropane molecules are first adsorbed in the inorganic corners of the MOFs at low pressures, then the organic linkers begin to adsorb molecules as the pressure increases. This is in good agreement with the results of inelastic neutron scattering (INS) and diffuse-reflectance IR spectroscopy.[7,30] It suggests that the predominant binding site is near the inorganic secondary build-

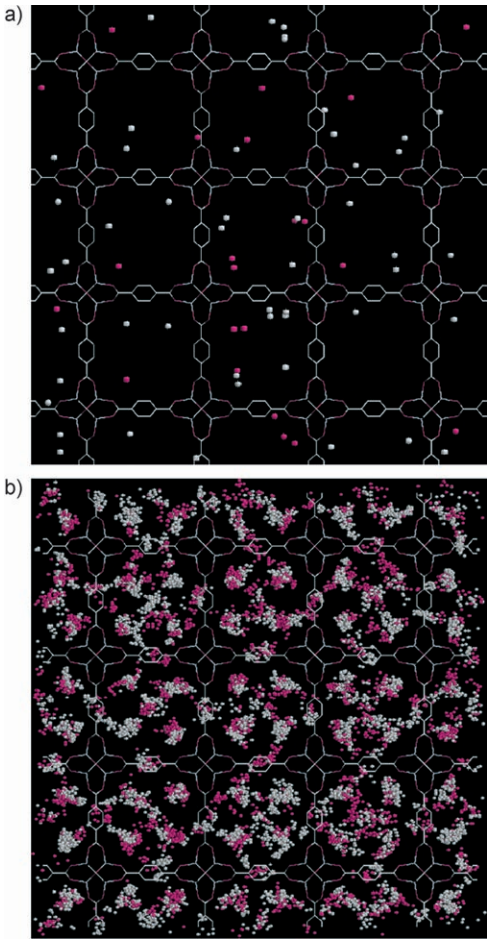

Figure 5. Probability distribution of 0.5/0.5 mixtures of *n*-butane (red)/2-methylpropane (white) at 298 K in IRMOF-1. a) 0.5×10^{-1} kPa, b) 0.5×10^{3} kPa.

ing units (SBUs). Owing to the large pore size, the *n*-butane and 2-methylpropane molecules are located around both the inorganic corners and the organic linkers. However, the amount adsorbed around the inorganic corners is slightly larger than that around the organic linkers in Figure 5b. This can be attributed to the stronger interaction between the metal/oxygen clusters and the alkane molecules. The probability distributions of *n*-butane and 2-methylpropane in IRMOF-6 at different pressures (Figure 6) are similar to those in IRMOF-1.

Interaction with the MOF framework: As discussed above, the interactions between the inorganic SBUs and the molecules must be stronger than that between the organic linkers and the molecules. To confirm this conclusion, a test alkane molecule (probe) was pushed through the center of the pore channel, and the averaged interaction energy between the alkane molecule and the IRMOF frameworks were calculated. A schematic view of the center-of-mass locus of the probe alkane molecule is shown in Figure 7. A series of points were equally partitioned along the y direction (L_y). The alkane molecule was put into the channel of the

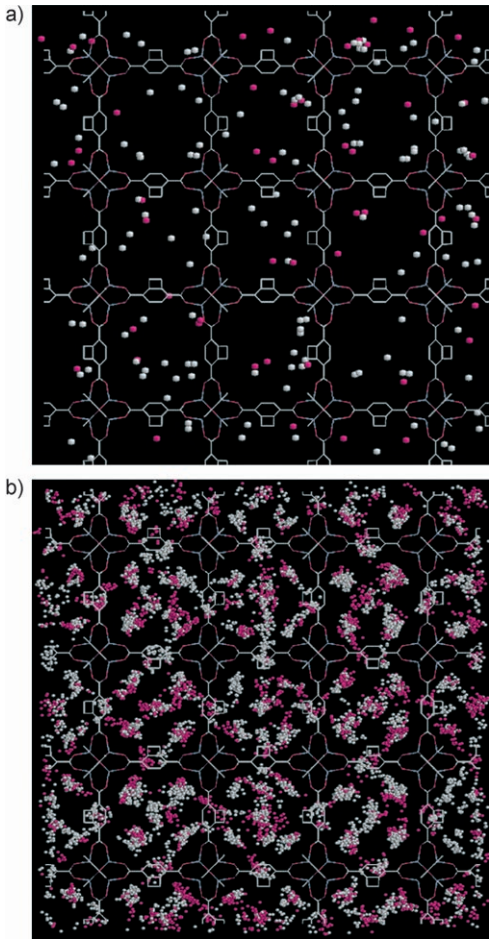

Figure 6. Probability distribution of 0.5/0.5 mixtures of *n*-butane (red)/2-methylpropane (white) at 298 K in IRMO-6. a) 0.5×10^{-1} kPa, b) 0.5×10^{3} kPa.

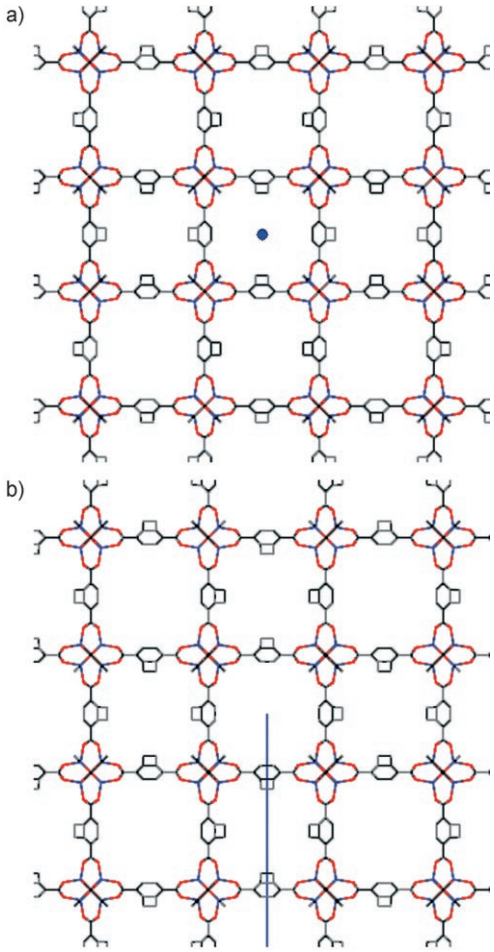

Figure 7. Skeletal drawings of the framework structure of IRMOF-6 with the center of mass of alkane molecules located at the center of the pore channel. Schematic views of the *xz* plane (a) and *yz* plane (b). The blue points represent the center of mass of the probe molecule.

IRMOFs, and the configuration of the molecule was optimized with 10^5 MC steps at each point. Then a lowest energy configuration was achieved. In this way, a series of configurations could be obtained. Finally, an optimal configuration was selected from these configurations by comparing the interaction energy. The configuration of the molecule was then fixed, and 10^5 MC cycles of rotation perturbation were performed for the alkane molecule at each point. In every cycle, the interaction energy was recorded to calculate the averaged interaction energy at the end.

As an example, the *n*-butane and 2-methylpropane probe molecules were pushed into the pore channel of IRMOF-6 (-1) at the center (about 25.8 Å in the *x* and *z* directions), respectively, as shown in Figure 7. The location in IRMOF-1 is similar to that in IRMOF-6. The calculated averaged energy between the probe molecule and the frameworks of IRMOF-1 (-6) are plotted in Figure 8. It was observed that the energy curve changes periodically with *y*, and no remarkable difference was found between Figure 8a and b. Thus the interactions between the adsorbate molecules at the center of the channel and the organic linker are not significant, and the organic linker influences the molecules adsorbed at the pore center weakly. The differences between peak and vale of the energy curves for both *n*-butane and 2-methylpropane are much larger than those in zeolites, that is, there are some preferred adsorption sites for adsorbate molecules. The vale of the energy curve indicates that the lowest energy for *n*-butane and 2-methylpropane is about -18 kJ mol^{-1}, located at 6.7 and 19.6 Å along the *y* axis. These positions are much closer to the two oxygen atoms of the Zn_4O cluster than the other positions. In other words, the closer to the Zn_4O cluster, the stronger the interaction between the frameworks and the adsorbed molecules, which agrees well with the probability distribution of *n*-butane and 2-methylpropane discussed above.

To further explore the role of the Zn_4O cluster during adsorption, *n*-butane and 2-methylpropane were pushed into IRMOF-6 (-1) at the position of about 1/4 of the pore channel (Figure 9, closer to the inorganic corner of the Zn_4O cluster, about 23.8 Å on the *x* and *z* axes). The averaged energy between probe alkane molecules and the frameworks is presented in Figure 10. The shapes of the energy curves for *n*-butane and 2-methylpropane in IRMOFs is different

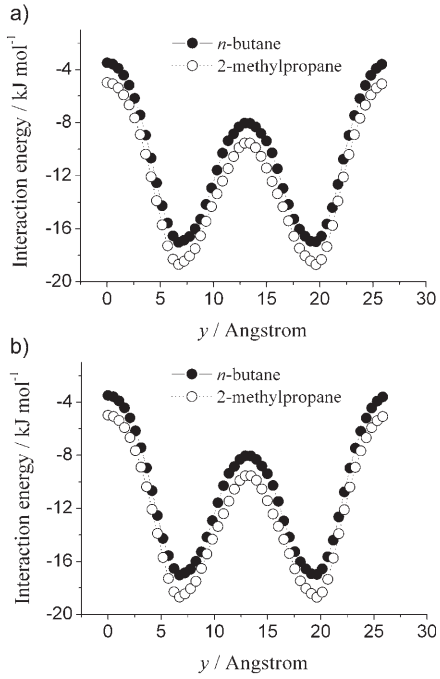

Figure 8. Averaged interaction energy between the IRMOFs and the adsorbate, calculated by using probe molecules of *n*-butane and 2-methylpropane at the center of the pore channel. a) IRMOF-1, b) IRMOF-6.

from those in Figure 8. The lowest energy for *n*-butane and 2-methylpropane in IRMOF-1 and IRMOF-6 is about $-23\ kJ\,mol^{-1}$, that is, $5\ kJ\,mol^{-1}$ lower than that in Figure 8, which suggests that the attractive interactions between the frameworks and the adsorbate molecules become stronger as the probe molecule approaches the Zn_4O cluster. As shown in Figure 10a and b, there are two peaks at 7.8 Å and 18.6 Å for 2-methylpropane and two relatively lower peaks at the same position for *n*-butane. The energy peak of 2-methylpropane is much higher than that of *n*-butane, which is attributed to the presence of the methyl group. When the methyl group of 2-methylpropane is close to the Zn_4O cluster, the repulsive interaction caused by spatial hindrance would become more significant. Owing to the strong hindrance between the methyl group and the Zn_4O cluster, as well as the hindrance of the organic linker in IRMOF-6, the highest energy for 2-methylpropane in IRMOF-6 is as high as $110\ kJ\,mol^{-1}$ (Figure 10b), which is positive and much higher than that in IRMOF-1. It suggests that the repulsive force becomes the dominant interaction between the frameworks and the adsorbate molecules, while the predominant interaction in Figure 8 is attractive. For *n*-butane, the peak energy in IRMOF-6 is positive ($16\ kJ\,mol^{-1}$), while the energy at the same position in IRMOF-1 is negative ($-18\ kJ\,mol^{-1}$). This change is caused by the hindrance of the organic linker of IRMOF-6. Due to the larger repulsive interaction between the branched-isomer molecules and the IRMOF-6 framework, it is difficult for the 2-methylpropane molecules to approach the Zn_4O cluster of IRMOF-6 closely.

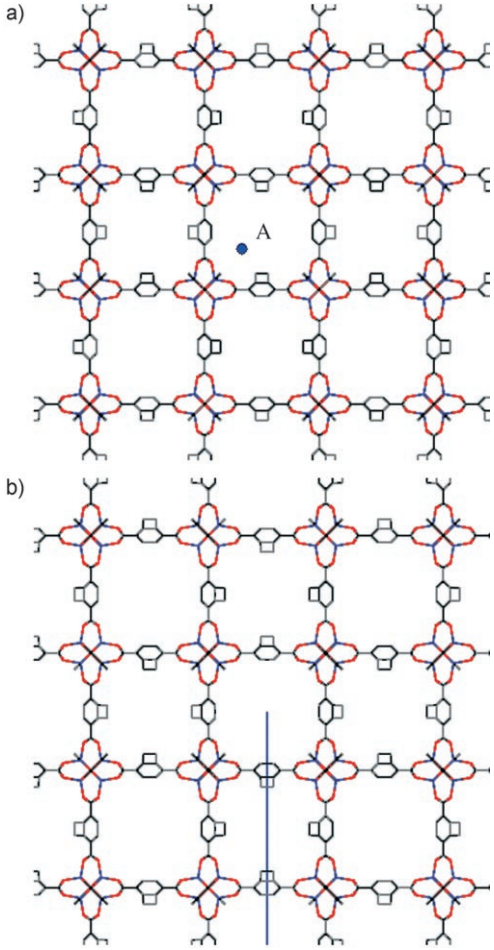

Figure 9. Skeletal drawings of the framework structure of IRMOF-6 with the center of mass of alkane molecules located at the position of about 1/4 of the pore channel. Schematic views of the *xz* plane (a) and *yz* plane (b). The blue points represent the center of mass of the probe molecule.

To elucidate this phenomenon, the 2-methylpropane molecule was also pushed into another pore channel (denoted as channel B) at the position of about 1/4 channel (Figure 11, 23.8 Å on the *x* axis and 10.9 Å at the *z* axis), and the pore channel that the probe molecule was pushed into in Figures 7 and 9 was denoted as channel A. The averaged interaction energies between the IRMOF-6 frameworks and the 2-methylpropane molecules pushed into pore channels A and B are plotted in Figure 12. There are two peaks at 5.7 and 20.7 Å along the *y* axis when 2-methylpropane is pushed through channel B, but at the same positions in channel A they have a minimum interaction energy, that is, they are at the vale of the energy curve. This interesting phenomenon can be attributed to the structure of the Zn_4O cluster. Two adsorption sites are located on one diagonal of the Zn_4O cluster, while another two equivalent adsorption sites are located on the other, and they lie in different planes. So when the probe molecule is pushed into channel A at the 5.7 and 20.7 Å on the *y* axis, it can interact with four adsorption sites, and the attractive interactions of the Zn_4O cluster to the adsorbate molecules become dominant.

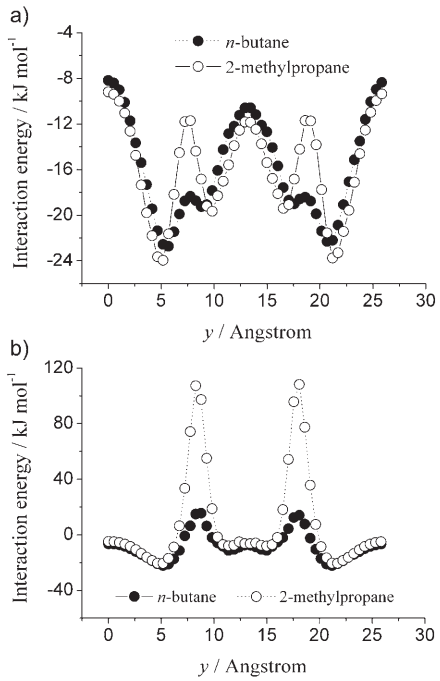

Figure 10. Averaged interaction energy between the IRMOFs and the adsorbate calculated by using probe molecules of *n*-butane and 2-methylpropane at the position of about 1/4 of the pore channel. a) IRMOF-1, b) IRMOF-6.

In contrast, at the same positions in channel B, no adsorption sites interact with the probe molecule, and the repulsive force caused by the spatial hindrance between the methyl group and the Zn_4O cluster, as well as the four side groups of the organic linker of IRMOF-6, become dominant. The stronger repulsive interaction between 2-methylpropane and IRMOF-6 is mainly caused by the hindrance between the methyl group and the side groups of the organic linker. The strong spatial hindrance is presumably the major reason why it is difficult for branched alkane molecules to closely approach the inorganic corners of IRMOF-6. In addition, the interaction energy curves also suggest that the larger the side groups, or the stronger the spatial hindrance, the more difficult it is for the branched alkane molecules approaching the Zn_4O cluster closely.

Adsorption behavior is determined by the Gibbs free energy of adsorption ($\Delta G = \Delta H - T\Delta S$), and the adsorption selectivity is dependent on the difference of ΔG between *n*-butane and 2-methylpropane, which is related to the adsorption enthalpy ΔH and adsorption entropy ΔS [Eq. (5)].

$$\Delta(\Delta G) = (\Delta G_{4n} - \Delta G_{4i}) = (\Delta H_{4n} - \Delta H_{4i}) - \mathrm{T}(\Delta S_{4n} - \Delta S_{4i}) \quad (5)$$

The interaction energy indicated that the adsorption enthalpy of branched alkanes is slightly larger than that of linear ones, which is in agreement with the studies of Martens et al.[31,32] They reported that methyl-branched isomers have lower adsorption enthalpy than linear molecules in the Henry regime or at low coverage when mixtures of alkane isomers are adsorbed in ZSM-22. They also suggested that the ability of a molecule to rotate in a cage can be estimated by the ratio R_g/R_c,[33] where R_g is the radius of gyration of its van der Waals volume, and R_c the radius of the largest sphere that fits into the van der Waals contour of the cage or pore. Owing to the shorter carbon backbone of the

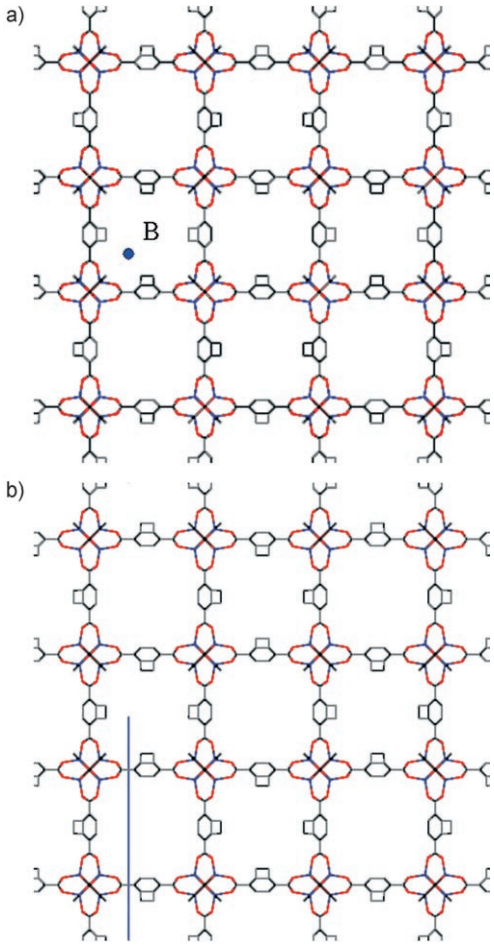

Figure 11. Skeletal drawings of the framework structure of IRMOF-6 with the center of mass of alkane molecules located at the position of about 1/4 of pore channel B. Schematic view of the *xz* plane (a) and *yz* plane (b). The blue points represent the center of mass of the probe molecule.

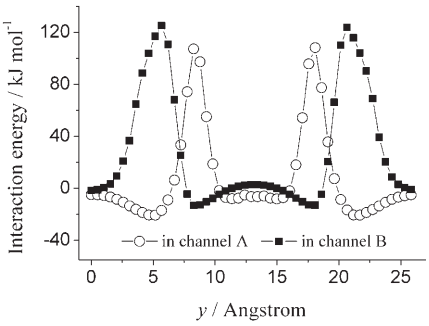

Figure 12. Averaged interaction energy between the adsorbate molecules and IRMOF-6 calculated by using a probe molecule of 2-methylpropane in channels A and B.

branched alkane, its radius of gyration is smaller than that of the corresponding linear alkane and it has a more spherical shape, so the branched alkane molecules can rotate more easily, which lead to their preferential adsorption in the pores.[33] However, due to the smaller alkane molecules and the larger pore sizes of IRMOFs, the rotation of *n*-butane is barely constrained, and thus the difference in rotational freedom between isomers is minor. Thus, when the alkane isomer mixtures are adsorbed in the pore channel, the value of $\Delta S_{4n}-\Delta S_{4i}$ is nearly zero, and the adsorption selectivity is mainly controlled by the adsorption enthalpy $\Delta H_{4n}-\Delta H_{4i}$. Therefore, the branched alkane molecules are preferentially adsorbed in the pore channel owing to its slightly larger adsorption enthalpy. However, as the alkane molecules approach the Zn_4O cluster of IRMOF-6 more closely (as shown in Figures 9 and 11), the rotational freedom of 2-methylpropane is hampered much more than that of *n*-butane owing to the spatial hindrance between the methyl group and the Zn_4O cluster and the side groups of the organic linker. Therefore, the adsorption entropy of 2-methylpropane ΔS_{4i} is larger than that of *n*-butane (ΔS_{4n}), and the value of ($\Delta S_{4n}-\Delta S_{4i}$) becomes notable, then the value of $-T(\Delta S_{4n}-\Delta S_{4i})$ would be more significant than the small value of ($\Delta H_{4n}-\Delta H_{4i}$). At this time, the straight chain alkanes are preferentially adsorbed at the Zn_4O cluster of IRMOF-6; in other words, the adsorption selectivity is mainly controlled by the adsorption entropy when the alkane molecules are close to the Zn_4O cluster.

In summary, the interactions between the Zn_4O cluster and the adsorbate are larger than that between the organic linker and the adsorbate, and the Zn_4O cluster plays the most important role during adsorption. Due to the spatial hindrance between the methyl group and side groups of the linker of IRMOF-6, it is difficult for branched alkane molecules to approach the Zn_4O clusters closely. When the mixtures of alkane isomer are adsorbed in the pore channels of IRMOF-6, the adsorption selectivity is mainly controlled by the adsorption enthalpy, but it is determined by the adsorption entropy when the alkane molecules are close to the Zn_4O cluster.

Dynamics: The dynamic behavior of adsorbate molecules in microporous materials is of great importance for understanding the adsorption mechanism. Adsorption is influenced by the dynamic behavior of the molecules, while the diffusion coefficients are also influenced by the adsorbed amount and the distribution of adsorbed molecules. To investigate the relationships between adsorption and dynamics, and to further explore the interesting phenomenon discussed above, in which it is difficult for branched alkanes to approach the Zn_4O cluster closely in IRMOF-6 compared with straight-chain alkanes, from the kinetic point of view, the diffusion coefficients of alkane isomer molecules were calculated by means of MD simulations. The configurations obtained from GCMC simulation were taken as the starting point. The self-diffusion coefficients of *n*-butane and 2-methylpropane with a loading of 20 molecules per unit cell in IRMOF-6 are 6.39×10^{-9} and 4.60×10^{-9} m^2s^{-1}, respectively, and they are smaller than those in IRMOF-1 with the same loading ($D_{4n}=9.34\times10^{-9}$, $D_{4i}=5.62\times10^{-9}$ m^2s^{-1}), which is attributed to the spatial hindrance of IRMOF-6. Owing to the presence of side groups in the organic linker of IRMOF-6, the rotational and translational degrees of freedom are reduced.[33] The number density profiles for *n*-butane and 2-methylpropane with a loading of 20 molecules per unit cell in IRMOF-6 were also investigated. Firstly, all the configurations of the simulation system were collected, and the profiles of *n*-butane and 2-methylpropane molecules in 3D space were statistically calculated. Then, by using an imaginary plane (about 10 Å thick) around the Zn_4O cluster, that is, at the positions 2–12 Å along the *z* axis, to cut the box, a tomographic image could be obtained by computer imaging. Finally, the image of the number density profile was obtained based on the statistically averaged result. The images here were averaged over all instantaneous configurations of 0.2×10^6 time steps (0.2 ns) after discarding 0.4×10^6 steps (0.4 ns). The images of the number density profiles for *n*-butane and 2-methylpropane around the Zn_4O cluster in IRMOF-6 are shown in Figure 13. The number density of *n*-

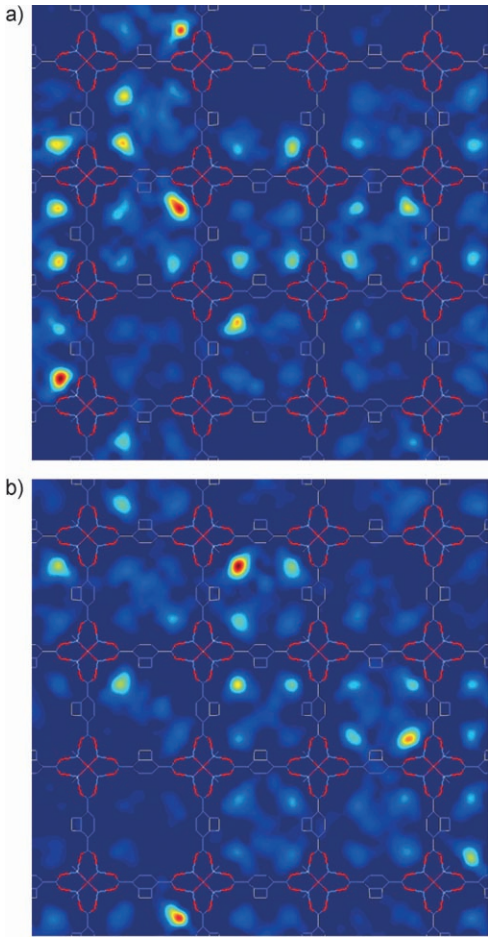

Figure 13. Images of number density distribution for alkane molecules adsorbed around the Zn_4O cluster: a) *n*-butane molecule, b) 2-methylpropane molecule.

butane around the Zn_4O cluster is slightly higher than that of 2-methylpropane, which illustrates that is hard for the 2-methylpropane molecules to approach the zinc sites owing to the spatial hindrance between 2-methylpropane and the side groups of the organic linker of IRMOF-6, as discussed above. However, this phenomenon was not observed in IRMOF-1. The number density profiles of *n*-butane around the Zn_4O cluster in IRMOF-1 are nearly the same as those of 2-methylpropane, and the density of the latter is even slightly larger than that of the former. In other words, the separation capability of IRMOF-6 is higher than that of IRMOF-1. This is consistent with the conclusion on selectivity discussed above. In addition, during the MD simulations, when the adsorbed molecules move close to one of the Zn_4O clusters of IRMOF-6, as shown in Figures 9 and 11, we calculated the residence time for one *n*-butane and one 2-methylpropane molecule, respectively. The residenc time for one *n*-butane molecule is about 0.356 ps within a simulation time of 0.6 ns. It is slightly longer than that of one 2-methylpropane molecule, which is about 0.292 ps. Although this only reflects the occupancy for alkane molecules around one Zn_4O cluster of IRMOF-6, due to the $Fm\bar{3}m$ symmetry of IRMOF-6, a similar residence time would be observed for an alkane molecule around another Zn_4O cluster. It further confirms that it is harder for long branched molecules to approach the Zn_4O cluster closely than for straight-chain alkane molecules.

Conclusion

A combination of the grand canonical Monte Carlo method and the configurational-bias Monte Carlo simulation technique was employed to study the adsorption behavior of mixtures of longer alkane isomers in IRMOFs. It was found that the adsorbed amounts of linear and branched alkanes increase with increasing pressure in IRMOF-1 and IRMOF-6, and the adsorbed amount of branched alkanes is larger than that of linear alkanes at higher pressures. Due to the larger pore size of IRMOFs, the storage capacities for alkane isomers are larger than those of most silicate zeolites. However, IRMOF-1 and IRMOF-6 have similar relative selectivities, and both of them are close to unity. The probability distribution of alkane molecules illustrates that they are first adsorbed at the Zn_4O clusters of the IRMOFs. Calculations of the interaction energy by means of molecular probes further confirmed that the Zn_4O cluster plays a much more important role than the organic linker during adsorption, and closer to the Zn_4O cluster the interaction between the frameworks and the adsorbed molecules is stronger. It was observed that it is difficult for branched alkane molecules to approach the inorganic corner of IRMOF-6 owing to the stronger repulsive interaction caused by spatial hindrance between the methyl group and the side groups of the linker. In addition, the absorption selectivity was investigated from the viewpoints of thermodynamics and kinetics. It is mainly controlled by the adsorption enthalpy when the alkane mixtures are adsorbed in the pore channels, but by the adsorption entropy when the alkane molecules are close to the Zn_4O cluster.

During MD simulation, the number density for *n*-butane around the Zn_4O cluster of IRMOF-6 is larger than that for 2-methylpropane, and the residence time for one *n*-butane molecule around the Zn_4O cluster is also slightly longer than that for 2-methylpropane. This is further indication that it is harder for branched alkane molecules to closely approach the Zn_4O cluster than for straight-chain molecules, from the kinetic viewpoint. In conclusion, this study demonstrates that GCMC and MD simulations are effective tools for seeking new candidates for hydrocarbon storage, and are helpful in locating the adsorption sites and understanding the adsorption mechanism in microporous materials.

Acknowledgement

This work was financially supported by the National Natural Science Foundation of China (Grant Nos. 20576112 and 50576080).

[1] M. Eddaoudi, J. Kim, N. Rosi, D. Vodak, J. Wachter, M. O'Keefe, O. M. Yaghi, *Science* **2002**, *295*, 469–472.
[2] O. M. Yaghi, M. O'Keefe, N. W. Ockwig, H. K. Chae, M. Eddaoudi, J. Kim, *Nature* **2003**, *423*, 705–714.
[3] T. Düren, R. Q. Snurr, *J. Phys. Chem. B* **2004**, *108*, 15703–15708.
[4] L. Pan, D. H. Olson, Ciemnolonski, L. R. Heddy, R. Li, *Angew. Chem.* **2006**, *118*, 632–635; *Angew. Chem. Int. Ed.* **2006**, *45*, 616–619.
[5] D. N. Dybtsev, A. L. Nuzhdin, H. Chun, K. P. Bryliakov, E. P. Talsi, V. P. Fedin, K. Kim, *Angew. Chem.* **2006**, *118*, 930–934; *Angew. Chem. Int. Ed.* **2006**, *45*, 916–920.
[6] R. Q. Snurr, J. T. Hupp, S. T. Nguyen, *AIChE J.* **2004**, *50*, 1090–1095.
[7] N. L. Rosi, J. Eckert, M. Eddaoudi, D. T. Vodak, J. Kim, M. O'Keeffe, O. M. Yaghi, *Science* **2003**, *300*, 1127–1129.
[8] P. M. Forster, J. Eckert, J-S. Chang, S-E Park, G. Férey, A. K. Cheetham, *J. Am. Chem. Soc.* **2003**, *125*, 1309–1312.
[9] J. L. C. Rowsell, A. R. Millward, K. S. Park, O. M. Yaghi, *J. Am. Chem. Soc.* **2004**, *126*, 5666–5667.
[10] B. Kesanli, Y. Cui, M. R. Smith, E. W. Bittner, B. C. Bockrath, W. Lin, *Angew. Chem.* **2004**, *117*, 74–77; *Angew. Chem. Int. Ed.* **2004**, *44*, 72–75.
[11] A. Vishnyakov, P. I. Ravikovitch, A. V. Neimark, M. Bulow, Q.-M. Wang, *Nano Lett.* **2003**, *3*, 713–718.
[12] A. I. Skoulidas, *J. Am. Chem. Soc.* **2004**, *126*, 1356–1357.
[13] A. I. Skoulidas, D. S. Sholl, *J. Phys. Chem. B* **2005**, *109*, 15760–15768.
[14] G. Garberoglio, A. I. Skoulidas, J. K. Johnson, *J. Phys. Chem. B* **2005**, *109*, 13094–13103.
[15] Q.-Y. Yang, C.-L. Zhong, *J. Phys. Chem. B* **2005**, *109*, 11862–11864.
[16] T. Düren, L. Sarkisov, O. M. Yaghi, R. Q. Snurr, *Langmuir* **2004**, *20*, 2683–2689.
[17] L. Sarkisov, T. Düren, R. Q. Snurr, *Mol. Phys.* **2004**, *102*, 211–220.
[18] L.-H. Lu, Q. Wang, Y.-C. Liu, *Langmuir* **2003**, *19*, 10617–10623.
[19] L.-H. Lu, Q. Wang, Y.-C. Liu, *J. Phys. Chem. B* **2005**, *109*, 8845–8851.
[20] T. J. H. Vlugt, W. Zhu, F. Kapteijn, J. A. Moulijn, B. Smit, R. Krishna, *J. Am. Chem. Soc.* **1998**, *120*, 5599–5600.
[21] S. L. Mayo, B. D. Olafson, W. A. Goddard III, *J. Phys. Chem.* **1990**, *94*, 8897–8909.
[22] W. L. Jorgensen, J. D. Madura, C. J. Swenson, *J. Am. Chem. Soc.* **1984**, *106*, 6638–6646.

[23] B. Smit, *J. Phys. Chem.* **1995**, *99*, 5597–5603.
[24] R. Krishna, D. Paschek, *Phys. Chem. Chem. Phys.* **2001**, *3*, 453–462.
[25] E. Beerdsen, D. Dubbeldam, B. Smit, T. J. H. Vlugt, S. Calero, *J. Phys. Chem. B* **2003**, *107*, 12088–12096.
[26] E. D. Akten, R. Siriwardane, D. S. Sholl, *Energy Fuels* **2003**, *17*, 977–983.
[27] E. Beerdsen, B. Smit, S. Calero, *J. Phys. Chem. B* **2002**, *106*, 10659–10667.
[28] J. Coronas, R. D. Noble, J. L. Falconer, *Ind. Eng. Chem. Res.* **1998**, *37*, 166–176.
[29] B. L. Chen, C. D. Liang, J. Yang, D. S. Contreras, Y. L. Clancy, E. B. Lobkovsky, O. M. Yaghi, S. Dai, *Angew. Chem.* **2006**, *118*, 74–77; *Angew. Chem. Int. Ed.* **2006**, *45*, 1390–1393.
[30] A. Zecchina, C. Otero Areán, *Chem. Soc. Rev.* **1996**, *25*, 187–197.
[31] J. A. Martens, G. Vanbutsele, P. A. Jacobs, J. Denayer, R. Ocakoglu, G. Baron, J. A. Munoz Arroyo, J. Thybaut, G. B. Marin, *Catal. Today* **2001**, *65*, 111–116.
[32] R. A. Ocakoglu, J. F. M. Denayer, G. B. Marin, J. A. Martens, G. V. Baron, *J. Phys. Chem. B* **2003**, *107*, 398–406.
[33] J. F. M. Denayer, R. A. Ocakoglu, I. C. Arik, C. E. A. Kirschhock, J. A. Martens, G. V. Baron, *Angew. Chem.* **2005**, *117*, 404–407; *Angew. Chem. Int. Ed.* **2005**, *44*, 400–403.

Received: February 5, 2007
Published online: May 16, 2007

